



journal homepage: <http://civiljournal.semnan.ac.ir/>

A New Relationship for Determining the Impact Force between Two Adjacent Structures Considering Building Pounding

Yaghub Ebrahimi¹, Alireza Mortezaei^{2*}, Ali Hemmati³, Mahmud Nikkhah Shahmirzadi³

1. Ph.D. Candidate, Civil Engineering Department, Semnan Branch, Islamic Azad University, Semnan, Iran

2. Associate Professor, Seismic Geotechnical and High Performance Concrete Research Centre, Civil Engineering Department, Semnan Branch, Islamic Azad University, Semnan, Iran

3. Assistant Professor, Seismic Geotechnical and High Performance Concrete Research Centre, Civil Engineering Department, Semnan Branch, Islamic Azad University, Semnan, Iran

Corresponding author: a.mortezaei@semnaniau.ac.ir

ARTICLE INFO

Article history:

Received: 15 March 2021

Revised: 01 January 2022

Accepted: 01 January 2022

Keywords:

Pounding;

Impact force;

Coefficient of restitution;

Spring stiffness;

Damping ratio.

ABSTRACT

Insufficient separation distance between two adjacent buildings can cause to collision when large lateral displacements are accrued due to seismic excitation. The impact force between structures induces many serious damages, which is called building pounding. In this study, pounding between two dynamic models is investigated and the impact force is numerically calculated. The impact is simulated based on special elements, including spring and dashpot, and the impact force and dissipated energy during the impact are determined. Both mentioned parameters depend significantly on the impact velocity, spring stiffness and the value of damping. For this purpose, the impact velocity of collision is parametrically measured and subsequently, coefficient of restitution is automatically determined. Furthermore, the impact damping ratio and nonlinear stiffness of spring are calculated to evaluate the impact between models. Finally, a new equation is presented to determine the value of damping and the accuracy of formula is confirmed, which is verified by three various approaches. In the first stage, an experimental test is considered and the peak impact force is extracted when a concrete ball is dropped on a rigid concrete surface. On the other hand, a numerical simulation is similarly assumed and the suggested formula is used to determine the peak impact force during collision. Then, the results of the peak impact forces between experimentally and numerically analyses are compared, which shows both are close to each other. Secondly, an estimated impact between two bodies has been studied. The results of the analysis are also compared between the dissipated and kinetic energies during impact. The comparisons indicate relatively low errors between the calculated and assumed values of the coefficient of restitution when the proposed equation is used. Finally, a value of the coefficient of restitution is selected and an impact is simulated to show hysteresis loop. The enclosed area of each loop is calculated as the dissipated energy and compared with the energy absorption. The above three comparisons show that the proposed formula is very effective and the accuracy of the impact force, calculated by the suggested formula as a parameter of the impact force model, is also acceptable.

How to cite this article:

Ebrahimi, Y., Mortezaei, A., Hemmati, A., Nikkhah Shahmirzadi, M. (2022). A New Relationship for Determining the Impact Force between Two Adjacent Structures Considering Building Pounding. *Journal of Rehabilitation in Civil Engineering*, 10(1), 141-155. <https://doi.org/10.22075/jrce.2022.22918.1493>

1. Introduction

Building pounding explains the collision between two structures, closed to each other, without gap or sufficient separation distance. Seismic excitation can naturally cause large lateral displacements of buildings, which is able to show serious damages even if buildings have been perfectly designed and excellently built. In fact, if the lateral displacements of buildings exceed their limitation of displacement, collision occurs between structures and elements damage or collapse. Separation distance between structures provides safety situation in order to avoid collision between them. Many researchers have focused on the philosophy of pounding to predict the values of the impact force and energy absorption due to external loading. For this challenge, special elements the included spring and dashpots, located at the level of contacts, are generally utilized to recognize collision and determine the impact force. Some researchers have experimentally investigated pounding and some other researchers numerically studied collision and also suggested many equations for the impact damping ratio. Papadrakakis and Mouzakis [1], Fillinfart et al. [2], Papadrakakis et al. [3], Shakya and Wijeyewickrema [4], Kajita et al. [5] and finally, Jankowski and Mahmoud [6] have carried out some experimental tests to evaluate pounding. They have considered different scaled models to set up and analyzed with static and dynamic loading. Some tests have implemented by different earthquake records to get the results of displacement and

pounding which shows the behavior of structures during earthquake in field of pounding. Masroor and Mosqueda [7] performed a series of earthquake simulator experiments to assess performance limit states of seismically isolated buildings under strong ground motions. Jankowski [8] presented the analysis of pounding between superstructure segments of a highway elevated bridge with three-span continuous deck under 3D non-uniform earthquake excitation and showed that the structural response depends largely on the gap size between adjacent segments. An experimental analysis has been recently carried out by Crozet et al. [9] which can be utilized as reference tests to be compared with the results of numerical analyses. On the other hand, Anagnostopoulos [10,11], Miari et al. [12], Jankowski [8,13], Komodromos [14,15], Ye et al. [16], Kun et al. [17], Barros et al. [18,19], Mahmoud et al. [20,21], Naderpour et al. [22–24], have numerically represented some equations to determine the impact damping ratio and calculate the impact force. For this purpose, they have simulated the impact and used different relations to calculate the impact damping ratio. However, significant differences can obviously be seen among the results of equations, considering the impact force and dissipated energy during the impact for different formulas. Other researchers have studied in zone of pounding and effect of plastic hinge length in building behaviour during earthquakes [25–27]. In this paper, a number of the above studies are explained and different equations are used to

compare the results of the peak impact force and dissipated energy. Hence, a new equation is needed to simulate collision and solve the equation of the impact. In fact, researchers have suggested different equations to calculate the impact velocity after collisions and also, the value of the impact damping ratio. Hence, it is vitally needed to predict and also describe a new equation to have mutual response in zone of impact damping ratio and also impact force with different situations. The main aim of this study is to predict the spring stiffness value using the coefficient of restitution and calculate the impact damping ratio to determine the impact force and dissipated energy with high accuracy, compared to other equations. For this purpose, a mathematically equivalent method based on the energy roll is considered and a new value of the impact velocity is logically estimated. The hysteresis curve of the impact is depicted and the enclosed area of the loop, occurring in each collision, is determined as the absorbed energy. According to the mathematical

$$\begin{cases} \bar{F}(\Delta t) = k\delta(\Delta t) + C_{imp}\dot{\delta}(\Delta t) \rightarrow linear \\ \bar{F}(\Delta t) = k_n\delta^{1.5}(\Delta t) + C_{imp}\dot{\delta}(\Delta t) \rightarrow nonlinear \end{cases} \quad (1)$$

where k is the stiffness of spring, C_{imp} denotes the impact damping and $\delta(\Delta t)$ and $\dot{\delta}(\Delta t)$ are the relative displacement and

$$\begin{cases} C_{imp} = 2.\bar{\zeta} \sqrt{k \frac{m_i m_j}{m_i + m_j}} \rightarrow linear \\ C_{imp} = 2.\bar{\zeta} \sqrt{k \sqrt{\delta(\Delta t)} \frac{m_i m_j}{m_i + m_j}} \rightarrow nonlinear \end{cases} \quad (2)$$

relations, a new value of the impact damping ratio is created and used to determine energy dissipation. On the other hand, dissipated energy is numerically calculated and compared with the energy absorption. Finally, if both of the energies become equal to each other, it shows that suggested the impact damping formula is able to calculate the impact force between buildings with acceptable accuracy. Consequently, the proposed formula can be used as a reference equation to determine damping ratio and the value of impact force during collision.

2. Past studies

Researchers have usually investigated the impact damping ratio in order to calculate the value of damping for determination of the impact force during collision. For this purpose, an impact is often simulated by conducting numerical analyses and an equation is generally used to calculate the impact force which is normally expressed as:

velocity, respectively. The differences among previous studies are the damping equations which are typically utilized to calculate energy dissipation and can be calculated by:

where m_i and m_j are the masses of the free bodies, $\bar{\zeta}$ is the impact damping ratio which depends significantly on the coefficient of restitution (e) and is typically defined as:

$$e = \frac{\dot{\delta}_A}{\dot{\delta}_I} \quad (3)$$

where $\dot{\delta}_A$ and $\dot{\delta}_I$ are the relative velocities after and before collision. However, the coefficient of restitution is used for $0 < e \leq 1$ and the plastic and elastic impacts correspond to $e = 0$ and $e = 1$, respectively.

As it was noted, many researchers have suggested different relationships to calculate the impact damping ratio which is defined by the coefficient of restitution and listed by the following expression.

- Anagnostopolos [10] was the first researcher who suggested the impact damping ratio for linear model:

$$\bar{\zeta} = -\frac{\ln(e)}{\sqrt{\pi^2 + (\ln(e))^2}} \quad (4)$$

$$\bar{\zeta} = e^{0.204} \frac{(1-e)}{e^{(\alpha+0.204)} + 3.351e\pi} \rightarrow \alpha = 1.05e^{0.653} \quad (8)$$

3. Proposed formula for impact force

In order to describe the building pounding and calculate the impact force as well as dissipated energy during collision, Equation (1) is considered and developed to three

- Mahmoud and Jankowski [20] have considered a linear model and represented an equation of motion for the impact damping ratio which can be explained as:

$$\bar{\zeta} = \frac{(1-e^2)}{e(e(\pi-2)+2)} \quad (5)$$

- Using Equation (5), Jankowski [13] has numerically modified the impact damping ratio formula by focusing on nonlinear model:

$$\bar{\zeta} = 4.5 \frac{\sqrt{5} \cdot (1-e^2)}{e(e(9\pi-16)+16)} \quad (6)$$

- Barros et al. [18] have suggested an equation of motion to calculate the impact damping ratio which can be described as:

$$\bar{\zeta} = \left(2 \frac{(1-e^2)}{e\sqrt{\pi}} \right)^2 \quad (7)$$

- Khatami et al. [24] have demonstrated the impact damping ratio formula based on a nonlinear model:

different parts. First part shows that spring and dashpot elements are activated when two bodies collide with each other and the results of the equation depend on the stiffness of spring, damping of dashpot, relative displacement and velocity [13]. In this part,

the impact force and dissipated energy are calculated. Then, the free bodies are naturally separated and the dashpot is automatically deactivated while the spring is still occupied.

$$\left\{ \begin{array}{l} \bar{F}(\Delta t) = k_n \delta^{1.5}(\Delta t) + C_{imp} \dot{\delta}(\Delta t) \rightarrow \delta > 0, \dot{\delta} > 0 \\ \bar{F}(\Delta t) = k_n \delta^{1.5}(\Delta t) \rightarrow \delta > 0, \dot{\delta} < 0 \\ \bar{F}(\Delta t) = 0 \rightarrow \delta > 0 \end{array} \right. \quad (9)$$

It seems that there are two unknown parameters that should be specified in order to solve Equation (9), which are k and C_{imp} .

Based on Equation (2) and in order to determine the value of the damping, the impact damping ratio ($0 \leq \bar{\zeta} \leq 1$) need to be obtained by the energy role.

$$\Delta E = 2\pi\bar{\zeta}_{imp} k \delta^2 = mgh \rightarrow gh = \frac{2\pi\bar{\zeta}_{imp} k \delta^2}{m} \quad (11)$$

$$\dot{\delta} = \sqrt{2gh} \rightarrow \dot{\delta} = \sqrt{\frac{4\pi\bar{\zeta}_{imp} k \delta^2}{m}} \quad (12)$$

Here ΔE is the dissipated energy during the impact. Thus,

$$\frac{1}{2} m \dot{\delta}_I^2 - 2\pi\bar{\zeta}_{imp} k \delta^2 = \frac{1}{2} m \dot{\delta}_A^2 \quad (13)$$

Using Equation (13) for finding the velocity after the impact, it would be written as:

$$\dot{\delta}_A = \sqrt{\dot{\delta}_I^2 - \frac{4\pi\bar{\zeta}_{imp} k \delta^2}{m}} \quad (14)$$

In order to provide a complete the impact, the relative velocity is assumed to be changed by

Finally, spring and dashpot are out of system. The mentioned parts of the impact to evaluate the pounding and calculate the impact force are suggested to be:

Considering a falling ball test, the dissipated energy is assumed to be equal to the elastic strain energy at the beginning of the impact which would be explained by:

$$mgh = \frac{1}{2} m \dot{\delta}^2 \quad (10)$$

a decreased coefficient for $\dot{\delta} > 0$ and also negative for $\dot{\delta} < 0$, which is given as follow:

$$\left\{ \begin{array}{l} \dot{\delta} = -\sqrt{\dot{\delta}_I^2 - \frac{4\pi\bar{\zeta}_{imp} k \delta^2}{m}} \rightarrow \dot{\delta} < 0 \\ \dot{\delta} = \mu e^{\beta} \cdot \sqrt{\dot{\delta}_I^2 - \frac{4\pi\bar{\zeta}_{imp} k \delta^2}{m}} \rightarrow \dot{\delta} > 0 \end{array} \right. \quad (15)$$

where μ and β are the model parameters obtained by fitting the experimental data using the method of the least squares ($\mu = 2.33$ and $\beta = 2.75$).

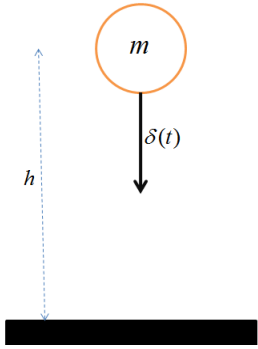


Fig. 1. Schematic of falling ball.

For experimentally verifying the obtained results from the analyses to determine the

mentioned parameters, an experimental test is carried out by a dropping ball from different heights (Fig 1). For this purpose, a 355 g ball is selected and dropped with zero velocity and impact velocity is calculated. Three different heights are assumed to be tested from 0.5 m to 3 m, by a 50 cm step. Then, the height of ball after collision is observed and listed to determine the velocity after impact. The results from the experimental tests are listed as follows:

Table 1. The value of impact velocities before and after the impact based on different height.

Hi(m)	0.5	1	1.5	2	2.5	3
Hj(m)	0.26	0.5	0.76	1.01	1.27	1.52
Vi(m/s)	3.13	4.43	5.43	6.26	7.00	7.67
Vj(m/s)	2.23	3.15	3.86	4.46	5.00	5.46

Here, Hi, Hj, Vi and Vj are the heights and velocities of the dropping ball before and after the collision, respectively. It can be seen that the value of the coefficient of restitution is approximately calculated to be 0.71. Hence, based on Equation (15) and the results for the velocities, an increased factor is assumed for

the impact velocity after collision. Using the recommended coefficient of restitution and a regression trend, the values of both unknown parameters are calculated as 2.33 and 2.75.

Furthermore, substituting Equation (12) and (15) into Equation (2), Equation (16) is generated by:

$$\Delta E = \int_0^{\delta_i} C_{imp} \dot{\delta} d\delta \rightarrow 2\bar{\zeta}_{imp} (2.33e^{2.75}) \sqrt{k \cdot m} \int_0^{\delta_i} \sqrt{\frac{4\pi\bar{\zeta}_{imp} k \delta_i^2}{m} - \frac{4\pi\bar{\zeta}_{imp} k \delta^2}{m}} d\delta \tag{16}$$

Equation (16) can be simplified by:

$$\Delta E = 2\bar{\zeta}_{imp} (2.33e^{2.75}) \cdot \sqrt{4\pi k^2 \bar{\zeta}_{imp}} \int_0^{\delta_i} \sqrt{\delta_i^2 - \delta^2} d\delta \tag{17}$$

By solving Equation (17), the kinetic energy can be expressed by Equation (18):

$$\Delta E = 4k \cdot \bar{\zeta}_{imp}^{1.5} (2.33e^{2.75}) \sqrt{\pi} (0.25\delta_i^2 \pi) \tag{18}$$

On the other hand, energy loss is considered to be equal to the kinetic energy which is:

$$\frac{1}{2} m (1 - e^2) \delta_A^2 = k \bar{\zeta}_{imp}^{1.5} (2.33e^{2.75}) \delta_i^2 \pi^{1.5} \tag{19}$$

Substituting Equation (12) in Equation (19) yields:

$$\frac{1}{2}m(1-e^2)\dot{\delta}_A^2 = k\bar{\zeta}_{imp}^{1.5}(2.33e^{2.75})\delta_I^2\pi^{1.5} \quad (20)$$

Simplifying Equation (20) yields:

$$(1-e^2)\dot{\delta}_A^2 = \sqrt{\bar{\zeta}_{imp}}\pi \frac{2.33e^{2.75}}{2}\dot{\delta}_I^2 \quad (21)$$

Finally, the impact damping ratio is generated as:

$$\bar{\zeta}_{imp} = \left(\frac{6(1-e^2)}{7\sqrt{\pi}e^{0.75}} \right)^2 \quad (22)$$

The results of the impact damping ratios are graphically shown in Figure 2. As it can be seen, there are decreasing trends in all models by increasing the coefficient of restitution. The impact damping ratio is suddenly changed from 7.269 to 0 when the coefficient of restitution changes from 0.1 to 1, respectively. As it was noted, the limitation of the impact damping ratio varies from 0 to 1, so $0.33 < e < 1.00$.

In here, it is assumed that the value of period is imitated from 0 to 1 s and structural damping ratio is also estimated to be 0 to 1. Another assumption is about energy dissipation, which is considered to be the area of hysteresis loop of each impact. In fact, energy dissipation has to be equal with energy absorption, calculated by equation (24). In order to calculate the impact force and determine the dissipated energy during the impact, coefficient of restitution is logically

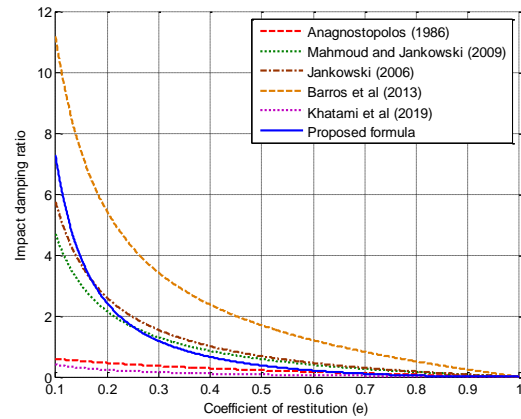


Fig. 2. Comparison of the relationship between the impact damping ratio and coefficient of restitution.

determined based on the impact velocity. Then, the impact damping ratio is numerically calculated for simulating the impact.

In order to evaluate the accuracy of the proposed relationship, three different strategies are considered and the accuracy of proposed formula is confirmed.

Firstly, an experimental test is used which has been performed by Jankowski and Mahmoud [6]. In this test, a ball with a specific mass (m) was dropped from different heights (h), on a rigid surface, considering same materials, and the impact forces were measured based on the time and the impact curve was graphically depicted. The impact has occurred in a short time with the maximum the impact force equal to 1194 N (Figure 3).

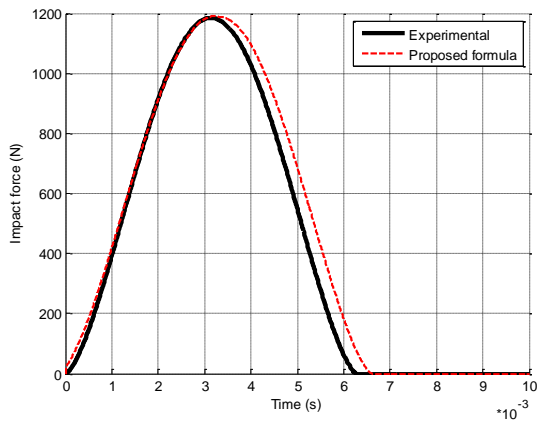


Fig. 3. The accuracy of proposed formula.

The results from the experimental tests are considered as the reference for comparing the results and evaluating the accuracy of the proposed relationship. Numerical analyses, using the proposed formula to calculate impact damping ratio, are carried out and the results are considered to compare with the experimental tests. The peak impact force from the numerical analysis is calculated as 1197 N, which shows an error below 1%. The results from the comparison indicate that the proposed formula can be used as the reference equation to calculate the values of the damping and consequently, the impact force during collisions.

Secondly, using the previous results in the field tests, difference values of the impact forces between the experimental tests and numerical analyses are considered, which are various from zero to 1200 N in different times. Impact force-time information have shown as a curve and compared with each experimental test as a reference. The results of

impact forces in mutual times are selected and an error for each step is calculated as:

$$Error(\%) = \frac{\sqrt{\sum_{i=0}^n (F_{ex} - F_{nu})^2}}{\sqrt{\sum_{i=0}^n F_{ex}^2}} \quad (23)$$

In this equation, F_{ex} and F_{nu} are the impact forces, determined from experimental tests and numerical analyses, respectively. The calculations of the errors are implemented for all models and compared with each other in Figure 4.

The results of solution for Equation (23) show that determining the impact force using Equation (7) and (4), presented by Barros et al. and Anagnostopolos, have the heights error among all used models, which are 16.8 and 16.4%, respectively. On the other hand, determining the impact force using Equations (8) and (22) has indicated the least errors about 13.8 and 13.7%. In fact, the proposed relationship has a high accuracy compared to other relationships.

Finally, in order to evaluate the last strategy for verifying the accuracy of the proposed formula, an assumed collision is simulated and the hysteresis loop of each impact is depicted. The enclosed area of the loop is calculated as the dissipated energy, which should be logically equal to the kinetic energy (Figure 5).

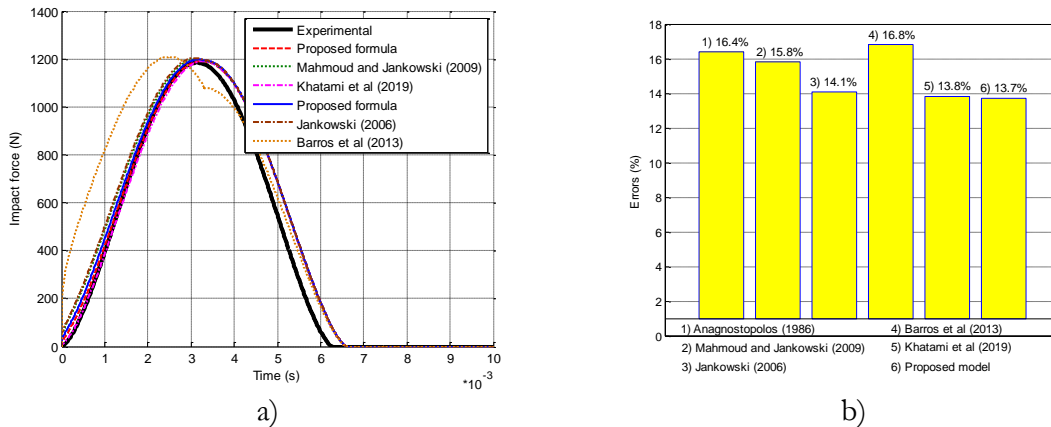


Fig. 4. Comparison of the results of a) Impact force and b) Calculated errors, for all models.

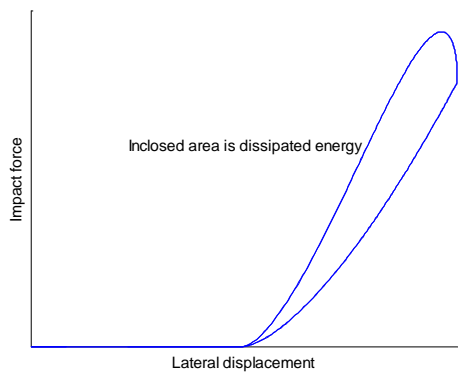


Fig. 5. Schematic curve of impact to show dissipated energy during impact.

For this purpose, an equal mass is considered to be 100 kg and the value of the impact velocity is changed from 1 to 50 m/s. The relationship between the impact force and relative displacement, which shows the dissipated energy and peak impact force, is calculated and also depicted. Different coefficients of restitution are calculated and simulation of the impact is numerically carried out. Dissipated energy is determined and compared with kinetic energy. If both of them are equal, the accuracy of the proposed relationship is confirmed. For instance, using

the impact velocity equal to 24 m/s, the coefficient of restitution is calculated to be 0.444. Furthermore, the simulation of the impact is performed, and then the equations are solved to determine the dissipated energy and kinetic energy, which are 255.53 and 257.32 N.m, respectively. Finally, the results are compared with each other to calculate the error for each simulation. The percentage errors of the dissipated energies are 0.7, 0.65, 0.58, 0.43, 0.37 and 0.22 for the coefficient of restitution equal to 0.4 to 0.9, respectively.

The evaluation results on the accuracy of the proposed relationship are depicted and compared with the utilized coefficient of restitution in Figure 6. It shows that the dissipated energy and the kinetic energy are close to each other and the simulation errors vary from 0.7% to 0.22% for the coefficient of restitution equal to 0.4 and 1, respectively. For instance, the dissipated energy is 373.5 N.m for the coefficient of restitution of 0.4, while the kinetic energy shows a value of 370.8 N.m which demonstrates an error of

0.7% between them. The results of the analyses indicate the accuracy of the suggested relationship. On the other hand, selected the coefficient of restitution (varying from 0.33 to 1) is used to calculate the damping ratio and then, the hysteresis loop of impact is depicted. The enclosed area of each loop is determined as the dissipated energy and the energy absorption is also calculated based on the energy role, which is written as follow:

$$E = 0.5.m.(1 - e^2).\dot{\delta}^2 \tag{24}$$

Dissipated energy and energy absorption are compared with each other. If both of them become the same this shows that the accuracy of the proposed formula can be confirmed. For this purpose, the selected coefficients of restitution are 0.33, 0.4, 0.5, 0.6, 0.7, 0.8, 0.9 and 1, giving the coefficient of restitution as 0.325, 0.38, 0.485, 0.59, 0.595, 0.7, 0.8, 0.9 and 1, respectively.

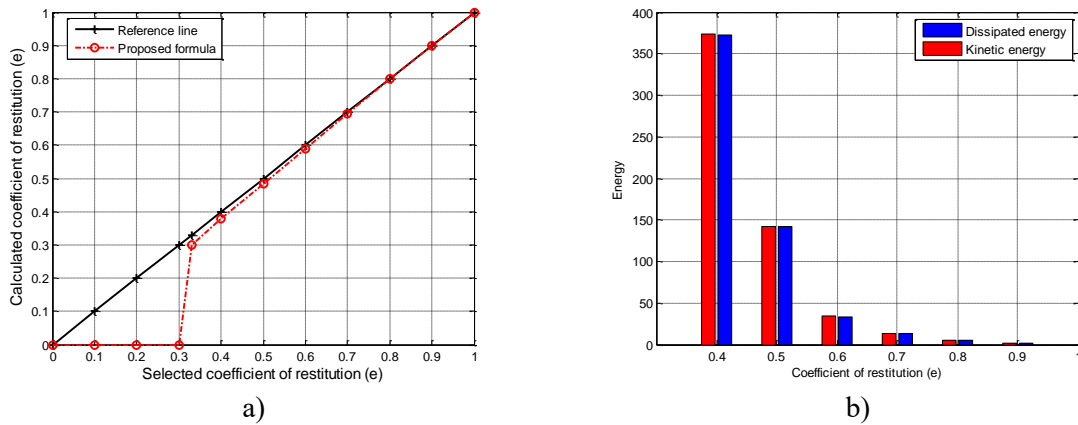


Fig. 6. The results of the analyses a) Comparison of the coefficient of restitution and b) Dissipated energy versus kinetic energy.

In order to evaluate the pounding phenomenon using the proposed relationship and investigate the effect of the impact damping ratio, damping and nonlinear spring stiffness, five ground motion records are selected, including those for Kobe (1995),

Tabas (1978), Sanfernando (1971), Loma Prieta (1995) and Elcentro (1940).

Earthquake records are logically selected to have magnitude from 6.6 to 7.4 by having different peak ground accelerations to study various situation with high and low PGAs.

Table 2. Properties of the selected earthquakes.

Earthquake	Date	Magnitude	Station	Component	PGA(cm/s ²)	PGV (cm/s)
Loma Prieta	17.10.1989	6.9	Corralitos	NS	631.51	44.7
Kobe	17.01.1995	7.2	JMA	NS	817.82	27.67
Tabas	16.09.1978	7.4	Tabas	NS	784.81	61.84
El Centro	18.05.1940	6.9	El Centro	NS	307.00	33.45
San Fernando	09.02.1971	6.6	Pacoima Dam	N16°W	1202.62	42.35

3.1. PGA – Peak Ground Acceleration

As it can be seen in Equation (22), the impact damping ratio depends normally on the coefficient of restitution and changes with different value of e . For this purpose, various coefficient of restitution are selected to conduct the simulation on the impact and calculate the impact force. In this challenge, building vibration period is assumed to be 0.5 s and the mass is also considered to be 10 kg while impact velocity is 21 m/s. Naturally, different coefficient of restitution calculate various impact damping ratio and subsequently, there are different damping value and impact forces. The results of the simulation are depicted in Figure 8 which shows that the peak impact force has occurred with 8924 N, 6795 N, 3876 N, 2832 N and 2106 N for the Kobe, Elcentro, Sanfernando, Tabas and Loma Prieta earthquakes, respectively.

All mentioned records are directly normalized to investigate the effect of earthquake properties when bodies collide with each other [23,24]. The scaled PGA of records is assumed to be 0.35g. The information of the utilized earthquakes is listed in Table 2.

4. Numerical studies

For this research, an assumed dynamic model is considered to investigate the value of the impact force during collision. Simulation of the impact is numerically conducted and the results of analyses are depicted in Figure 7. It can be obviously observed that the largest response in zone of the impact force is found for the Elcentro earthquake with a peak impact force equal to 17.12 N, and then, Sanfernando, Kobe, Tabas and finally, Loma

Prieta with the peak the impact forces equal to 13.38, 8.25, 6.13 and 4.78 N, respectively.

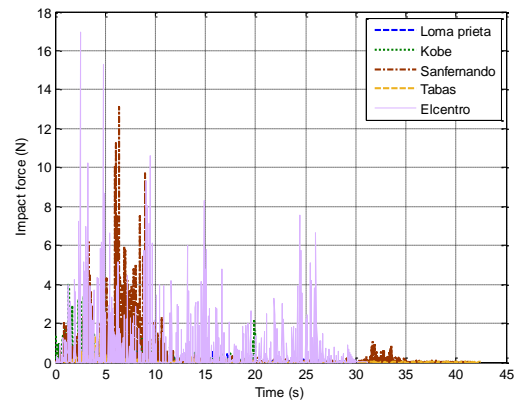


Fig. 7. Comparison of the peak impact forces for the utilized records.

4.1. Effect of the coefficient of restitution

As it is obviously seen, peak impact force is decreased to zero by decreasing coefficient of restitution because impact damping ratio is declined, which is caused to reduce damping value and subsequently, impact force is decreased.

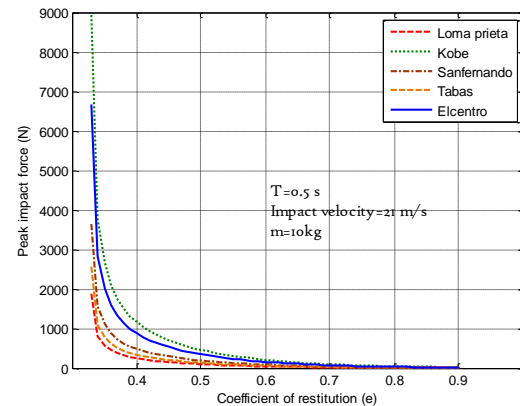


Fig. 8. Comparison of the peak impact forces for the utilized records.

4.2. Effect of the natural period

Considering different natural periods of the used dynamic model, the peak impact forces are calculated based on various periods, obtained from 0 to 1 second. The limitation

of period is selected based on an assumption and can be changed to more value of period. It can be seen in Figure 9 that models have shown slow increase trends for Kobe, Elcentro and Sanfernando earthquakes which have peak displacements equal to 12.2, 25.5 and 25.6 N, respectively.

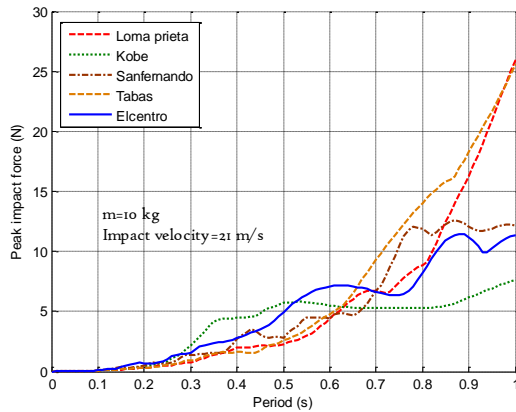


Fig. 9. Comparison of the peak impact forces with period for different utilized records.

On the other hand, the peak impact forces for the Loma Prieta and Tabas earthquake records have indicated a suddenly increase from 0 to 3 seconds and then, there is a normal decrease for the Tabas earthquake records and a sharp grow to for the Loma Prieta earthquake records. The largest and lowest the impact forces are 17.65 and 12.2 N for the Loma Prieta and Kobe earthquake records, respectively. Reduction of period is caused to decrease lateral displacement and also decline impact force between bodies.

4.3. Effect of the structural damping ratio

The effect of the structural damping ratio is evaluated to find the peak impact force. The structural damping ratio is assumed to be from 0 to 1%. As it can be seen in Figure 9, there is a slow decline in the dynamic model for all earthquake records. In other words, increasing structural damping ratio will decrease the peak impact force. The values of

the dominate peak impact forces are 197 and 725 N for Tabas and Elcentro earthquakes, which are normally reduced to 53 and 75 N for the structural damping ratio equal to 1. It shows that increasing the structural damping ratio is able to enhance the stiffness of the model and subsequently, decrease the lateral displacement and the peak impact force.

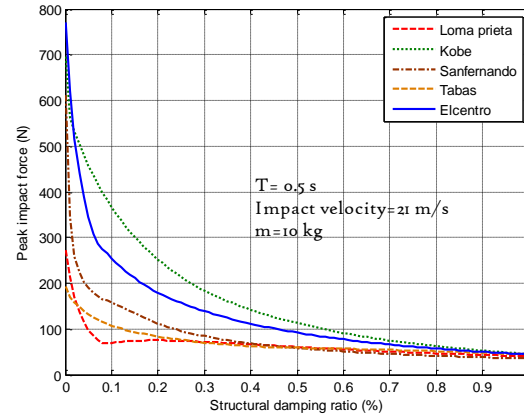


Fig. 10. Comparison of the peak impact force.

As it was noted in 3.1, decreasing structural damping ratio is caused to decline impact force.

4.4. Effect of the gap size

Examining the effect of separation distance between two adjacent models shows that by increasing the gap size, the peak impact force declines. For this purpose, a critical distance is considered to be 0 to 1 mm between the analyzed models. The peak impact forces are 99, 138, 191, 346 and 458 N for the Loma Prieta, Tabas, Sanfernando, Elcentro and Kobe earthquake records, respectively. When the limitation of gap size exceeds 3 mm, there are no any impact forces for the Loma Prieta, Tabas and Sanfernando earthquake records. However this is between 5 and 6 mm for the Elcentro and Kobe earthquakes, respectively (Figure 11).

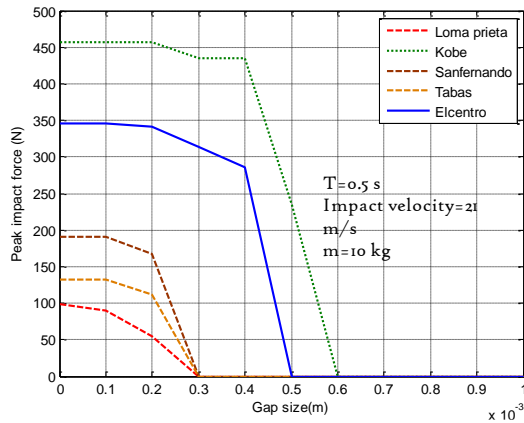


Fig. 11. Comparison of the peak impact forces based on the gap size for the utilized records

Providing sufficient gap size between buildings and increase it is caused to avoid collisions and also reduce impact force during seismic excitations.

5. Conclusions

Large lateral displacement between two adjacent structures causes contact and pounding. The authors have numerically suggested different equations to calculate the impact damping ratio for determining the impact force and dissipated energy during the impact. In this study, a new relationship between the motion in the zone of the impact, damping ratio was suggested. For this purpose, using a mathematical process and energy role, a new equation in zone of damping ratio is created. The accuracy of the proposed relationship was evaluated at different levels and also approved. In order to investigate the accuracy of the proposed formula, three different strategies are considered based on experimental and numerical analyses. In this paper, the impact velocity was considered as an input and the coefficient of restitution was determined. Furthermore, the impact damping ratio is mathematically suggested and the impact force were calculated. In order to evaluate

the effect of time, the coefficient of restitution, period, structural damping and gap size on the suggested relationship, the peak impact forces were determined based on five earthquake records. The results showed that increasing the coefficient of restitution, structural damping and gap size causes the impact force to decrease among all the selected records which are shown in the figures. On the contrary, by increasing the period of structures, the lateral displacement of buildings is naturally increased and subsequently, increases the impact force. For example, increasing coefficient of restitution is caused to decrease impact force from 8924 to zero by using Kobe earthquake record. It is mentioned that decreasing structural damping value has reduced impact force from 725 to zero by considering Elcentro earthquake record and finally, increasing gap size between models has been prevented collisions and decreased impact force from 458 to zero by using Kobe earthquake record.

REFERENCES

- [1] Papadrakakis M, Mouzakis HP. Earthquake simulator testing of pounding between adjacent buildings. *Earthq Eng Struct Dyn* 1995;24:811–34. <https://doi.org/10.1002/eqe.4290240604>.
- [2] Filiatrault A, Wagner P, Cherry S. Analytical prediction of experimental building pounding. *Earthq Eng Struct Dyn* 1995;24:1131–54. <https://doi.org/10.1002/eqe.4290240807>.
- [3] Papadrakakis M, Mouzakis H, Plevris N, Bitzarakis S. A lagrange multiplier solution method for pounding of buildings during earthquakes. *Earthq Eng Struct Dyn* 1991;20:981–98. <https://doi.org/10.1002/eqe.4290201102>.
- [4] Shakya K, Wijeyewickrema AC. Mid-Column Pounding of Multi-Story Reinforced Concrete Buildings considering Soil Effects. *Adv Struct Eng* 2009;12:71–

85.
<https://doi.org/10.1260/136943309787522687>.
- [5] Kajita Y, Kitahara T, Nishimoto Y, Otsuka H. Estimation of maximum impact force on natural rubber during collision of two steel bars. 1st Eur. Conf. Earthq. Eng. Seismol. (1st ECEES), Geneva, Switzerland, Sept., 2006, p. 3–8.
- [6] Jankowski R, Mahmoud S. Linking of adjacent three-storey buildings for mitigation of structural pounding during earthquakes. *Bull Earthq Eng* 2016;14:3075–97.
<https://doi.org/10.1007/s10518-016-9946-z>.
- [7] Masroor A, Mosqueda G. Experimental simulation of base-isolated buildings pounding against moat wall and effects on superstructure response. *Earthq Eng Struct Dyn* 2012;41:2093–109.
<https://doi.org/10.1002/eqe.2177>.
- [8] Jankowski R. Pounding Between Superstructure Segments in Multi-Supported Elevated Bridge with Three-Span Continuous Deck Under 3D Non-Uniform Earthquake Excitation. *J Earthq Tsunami* 2015;09:1550012.
<https://doi.org/10.1142/S1793431115500128>.
- [9] Crozet V, Politopoulos I, Chaudat T. Shake table tests of structures subject to pounding. *Earthq Eng Struct Dyn* 2019;48:1156–73.
<https://doi.org/10.1002/eqe.3180>.
- [10] Anagnostopoulos SA. Pounding of buildings in series during earthquakes. *Earthq Eng Struct Dyn* 1988;16:443–56.
<https://doi.org/10.1002/eqe.4290160311>.
- [11] Anagnostopoulos SA. Equivalent viscous damping for modeling inelastic impacts in earthquake pounding problems. *Earthq Eng Struct Dyn* 2004;33:897–902.
<https://doi.org/10.1002/eqe.377>.
- [12] Miari M, Choong KK, Jankowski R. Seismic pounding between adjacent buildings: Identification of parameters, soil interaction issues and mitigation measures. *Soil Dyn Earthq Eng* 2019;121:135–50.
<https://doi.org/10.1016/j.soildyn.2019.02.024>.
- [13] Jankowski R. Non-linear viscoelastic modelling of earthquake-induced structural pounding. *Earthq Eng Struct Dyn* 2005;34:595–611.
<https://doi.org/10.1002/eqe.434>.
- [14] Komodromos P, Polycarpou PC, Papaloizou L, Phocas MC. Response of seismically isolated buildings considering poundings. *Earthq Eng Struct Dyn* 2007;36:1605–22.
<https://doi.org/10.1002/eqe.692>.
- [15] Komodromos P, Polycarpou P. On the numerical simulation of impact for the investigation of earthquake-induced pounding of building. Tenth Int. Conf. Comput. Struct. Technol. Civil-Comp Press. Stirlingshire, Scotl., 2010.
- [16] Ye K, Li L, Zhu H. A note on the Hertz contact model with nonlinear damping for pounding simulation. *Earthq Eng Struct Dyn* 2009;38:1135–42.
<https://doi.org/10.1002/eqe.883>.
- [17] Kun C, Yang Z, Chouw N. Seismic response of skewed bridges including pounding effects. *Earthquakes Struct* 2018;14:467–76.
- [18] Barros RC, Naderpour H, Khatami SM, Mortezaei A. Influence of Seismic Pounding on RC Buildings with and without Base Isolation System Subject to Near-Fault Ground Motions. *J Rehabil Civ Eng* 2013;1:39–52.
<https://doi.org/10.22075/jrce.2013.4>.
- [19] Naderpour H, Barros RC, Khatami SM. A new model for calculating impact force and energy dissipation based on the CR-factor and impact velocity. *Sci Iran* 2015;22:59–68.
- [20] Mahmoud S, Chen X, Jankowski R. Structural Pounding Models with Hertz Spring and Nonlinear Damper. *J Appl Sci* 2008;8:1850–8.
<https://doi.org/10.3923/jas.2008.1850.1858>.
- [21] Mahmoud S, Jankowski R. Modified linear viscoelastic model of earthquake-induced structural pounding. *Iran J Sci Technol*

- Trans Civ Eng 2012;35:51–62.
<https://doi.org/10.22099/ijstc.2012.656>.
- [22] Naderpour H, Barros RC, Khatami SM, Jankowski R. Numerical Study on Pounding between Two Adjacent Buildings under Earthquake Excitation. *Shock Vib* 2016;2016:1–9.
<https://doi.org/10.1155/2016/1504783>.
- [23] Naderpour H, Khatami SM, Barros RC. Prediction of critical distance between two MDOF systems subjected to seismic excitation in terms of artificial neural networks. *Period Polytech Civ Eng* 2017;61:516–29.
<https://doi.org/10.3311/PPci.9618>.
- [24] Khatami SM, Naderpour H, Barros RC, Jakubczyk-Gałczyńska A, Jankowski R. Effective Formula for Impact Damping Ratio for Simulation of Earthquake-induced Structural Pounding. *Geosciences* 2019;9:347.
<https://doi.org/10.3390/geosciences9080347>.
- [25] Xu X, Xu X, Liu W, Zhou D. A New Formula of Impact Stiffness in Linear Viscoelastic Model for Pounding Simulation. *Shock Vib* 2016;2016:1–7.
<https://doi.org/10.1155/2016/5861739>.
- [26] Mortezaei A, Ronagh HR. Effectiveness of modified pushover analysis procedure for the estimation of seismic demands of buildings subjected to near-fault ground motions having fling step. *Nat Hazards Earth Syst Sci* 2013;13:1579–93.
<https://doi.org/10.5194/nhess-13-1579-2013>.
- [27] Mortezaei A. Plastic hinge length of RC columns considering soil-structure interaction. *Earthquakes Struct* 2013;5:679–702.
<https://doi.org/10.12989/eas.2013.5.6.679>.